BULLETIN OF THE POLISH ACADEMY OF SCIENCES
TECHNICAL SCIENCES, Vol. 73(4), 2025, Article number: e153223
DOI: 10.24425/bpasts.2025.153223



# Slip compensation technique in five-phase induction motors drive system

**Krzysztof BLECHARZ[1]*, Roland RYNDZIONEK[1], Paul GONDRAN[2], and Imad MERZOUK[3]**

[1] Gdansk University of Technology, Faculty of Electrical and Control Engineering, ul. Narutowicza 11/12, 80-233 Gdansk, Poland
[2] Novatem SAS, 20 avenue Didier DAURAT, 31400 Touluse, France
[3] Djelfa University, Laboratory of Applied Automation and Industriual Diagnosis, 17000 Djelfa, Algeria

**Abstract.** The article presents a slip compensation method for traditional scalar (V/f) control of a five-phase induction motor. The proposed control method uses the possibility of injecting the third harmonic of voltage to increase the motor's electromagnetic torque. The solution is characterized by both the simplicity of scalar control and improved speed control efficiency. The paper presents the PLECS simulation results and describes the laboratory tests that were conducted. Several scenarios were performed with dedicated and self developed algorithm in a laboratory stand using a five-phase induction motor.

**Keywords:** five-phase induction motor; multi-phase motor; open-loop control; slip compensation; scalar control.

## 1. INTRODUCTION

In light of the global energy crisis, it is becoming increasingly clear that there is a need for more energy-efficient electromagnetic conversion systems. In order to address the challenges posed by global and local pollution, the depletion of fossil fuels, and higher gas prices, it would be beneficial to consider ambitious plans for new residential and industrial appliances and machines with less energy consumption [1–6]. Consequently, researchers are currently concentrating their efforts on the development of devices with enhanced energy efficiency and a minimal carbon footprint.

Due to their cost-effectiveness and robust construction, induction motors are utilized extensively in both industrial and domestic settings [7]. One of the primary advantages of the induction motor is its mechanical simplicity, which contributes to its widespread applicability.

The development of multiphase machines is common in a range of fields related to motors and generators [8–11]. Multiphase electric drives are the focus of research for the improvement of industrial technologies such as fans and pumps. In addition, there is an opportunity to increase the number of phases by increasing the number of legs with the advent and flexible use of high-power semiconductor devices in inverter drives for power applications [12, 13]. In general, the multi-phase machine has several advantages over the classical three-phase machine. These include less torque ripple, greater fault tolerance, higher torque density, reduction of switches used in the inverter legs (lower current per phase for the same phase voltage and power), improved noise characteristics, and flat torque [14]. However, the main disadvantages of five phase machines are higher switching losses and more complex control algorithms due to the higher number of phases.

This induction machine is a significant competitor to the three-phase induction motor due to the possibility of torque increase through third harmonic injection combined with high robustness. In five-phase drives, torque can be improved by injecting the [15, 16].

Moreover, the control system allows the 1st and 3rd stator voltage harmonic components to be controlled independently. Therefore, two synchronized voltage sources for stator voltage component $u_{s\alpha}, u_{s\beta}, u_{sx}, u_{sy}$ generation for each mathematical plane in orthogonal frames are required to implement a 3rd harmonic injection drive.

This paper introduces and elaborates on the slip compensation method for traditional scalar (*V/f*) control of an induction motor. The focus is on the five-phase induction motor drive, with its general structure showcased in Fig. 1. Furthermore, this modification of scalar control method is new and it has been developed from a classical three-phase system and implemented for modern five-phase drives.

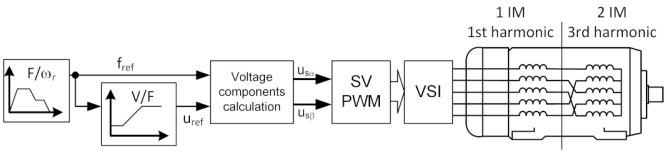


**Fig. 1.** Schematic diagram of the drive system with five-phase induction motor

## 2. MODEL OF FIVE-PHASE INDUCTION MOTOR

In this system, a five-phase induction motor is used. Generally, a five-phase induction motor can be represented as two independent virtual machines supplied by a single five-phase voltage or

*e-mail: krzysztof.blecharz@pg.edu.pl

Manuscript submitted 2024-09-02, revised 2024-11-06, initially accepted for publication 2024-12-04, published in July 2025.

current source. The presented solution uses a five-phase voltage inverter, which can be considered a fully regulated five-phase power source. A common drive shaft physically connects these machines.

Based on the classical model of a three-phase induction machine in steady states [17] was used to determine the five-phase model. An assumption has been made. It has been assumed that only the fundamental harmonic of the motor supply voltage is responsible for the average electromagnetic torque of the motor. This assumption was based on the observation that the rotating magnetic field from the higher rotating harmonic of the motor voltage has a very high speed. Furthermore, it has been assumed that all electrical energy losses occurring in the rotor from higher rotating harmonics are dissipated as thermal energy within the rotor cage. It should be noted that some losses are converted to heat in the rotor core by eddy currents; however, this has been neglected to simplify the model. A review of the literature reveals that third harmonic injection in a multi-phase system has the potential to reduce overall losses. In instances where higher torque demands are placed upon the system, the third harmonic field serves to mitigate the effects of iron saturation that would otherwise be caused by the basic field. This results in a reduction of overall losses. The combined influence of the basic field and the third harmonic field enables a modest reduction in losses, amounting to approximately 3–10%. Careful design and analysis are required to ensure that the benefits of third harmonic injection are realized in a five-phase induction motor. The five-phase induction motor system could be represented as two machines with phase transpositions that are independent of each other, as mentioned earlier. The equivalent circuits of the five-phase induction motor in the two orthogonal mathematical planes are shown in Fig. 2. Based on the simplified assumptions for the fixed orthogonal plane on the stator side [18], the model of the induction motor can be described as follows [19]:

$$\mathbf{u}_s^{(i)} = \mathbf{R}_s^{(i)}\mathbf{i}_s^{(i)} + \frac{\mathrm{d}\Psi_s^{(i)}}{\mathrm{d}\tau} + \mathrm{j}\omega_a\Psi_s^{(i)}, \tag{1}$$

$$0 = \mathbf{R}_{r(i)}\mathbf{i}_{r(i)} + \frac{\mathrm{d}\Psi_{r(i)}}{\mathrm{d}\tau} + \mathrm{j}\left(\omega_a - \omega_{r(i)}\right)\Psi_{r(i)}, \tag{2}$$

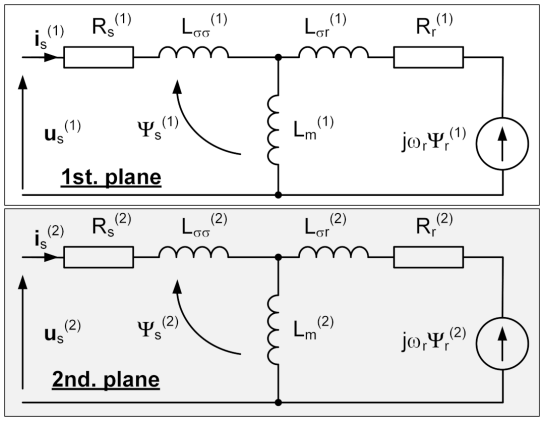


**Fig. 2.** Schematic diagram of the drive system with five-phase induction motor

$$\Psi_{1(i)} = \mathbf{L}_{1(i)}\mathbf{i}_{1(i)} + \mathbf{L}_{m1(i)}\mathbf{i}_{r(i)}, \tag{3}$$

$$\Psi_{2(i)} = \mathbf{L}_{2(i)}\mathbf{i}_{2(i)} + \mathbf{L}_{m2(i)}\mathbf{i}_{r(i)}, \tag{4}$$

$$\mathrm{J}\frac{\mathrm{d}\omega_r}{\mathrm{d}\tau} = \frac{3}{2}\mathrm{p}_1\mathrm{Im}\left|\Psi_{1(i)}^{*}\mathbf{i}_{1(i)}\right| + \frac{5}{2}\mathrm{p}_2\mathrm{Im}\left|\Psi_2^{(i)}\mathbf{i}_{2(i)}^{*}\right| - \mathrm{T}_{\mathrm{drive}}, \tag{5}$$

where $\Psi_s^{(i)}$, $\mathbf{i}_1^{(i)}$, $\mathbf{u}_{1(i)}$ and $\Psi_{r(i)}$, $\mathbf{i}_{r(i)}$ and $\Psi_r^{(i)}$, $\mathbf{i}_{2(i)}$, $\mathbf{u}_{2(i)}$ are the stator and rotor space vectors of magnetic fluxes, circuit currents and voltage for each mathematical plane, respectively. The superscript ($i = 1, 2$) defines the sets of state variable equations for two independent mathematical planes of state variables 1 and 2. Assuming that $\omega_a = \omega_{s1}$ for the first mathematical planes and $\omega_a = \omega_{s2}$ for the second machine and orienting stator fluxes accordingly with the d-axis at each plane is easy to write as follows:

For first virtual motor (1st plane)

$$\Psi_{sd}^{(1)} = \left|\Psi_s^{(1)}\right|, \qquad \Psi_{sq}^{(1)} = 0, \tag{6}$$

$$u_{sd}^{(1)} = R_s^{(1)}i_{sd}^{(1)} + \frac{\mathrm{d}\Psi_{sd}^{(1)}}{\mathrm{d}\tau}, \quad u_{sq}^{(1)} = R_s^{(1)}i_{sq}^{(1)} + \omega_{s1}\Psi_{sd}^{(1)}. \tag{7}$$

For second virtual motor (2nd plane)

$$\Psi_{sd}^{(2)} = \left|\Psi_s^{(2)}\right|, \quad \Psi_{sq}^{(2)} = 0, \tag{8}$$

$$u_{sd}^{(2)} = R_s^{(2)}i_{sd}^{(2)} + \frac{\mathrm{d}\Psi_{sd}^{(2)}}{\mathrm{d}\tau}, \quad u_{sq}^{(2)} = R_s^{(2)}i_{sq}^{(2)} + \omega_{s2}\Psi_{sd}^{(2)}. \tag{9}$$

where $\omega_{s1}$, and $\omega_{s2}$ are synchronous speeds for each plane. In the scalar method of controlling an induction motor, the dependencies of the control variables are based on the machine equations in a steady state as follows:

$$\frac{\mathrm{d}}{\mathrm{d}\tau}\left|\Psi_s^{(1)}\right| = 0, \qquad \frac{\mathrm{d}}{\mathrm{d}\tau}\left|\Psi_s^{(2)}\right| = 0. \tag{10}$$

The modules of the stator voltage vectors $u_s^{(1)}$ and $u_s^{(2)}$, for both mathematical planes in the steady state have the form:

$$\begin{aligned}\left|\mathbf{u}_s^{(1)}\right| &= \sqrt{\left(R_s^{(1)}i_{sd}^{(1)}\right)^2 + \left(R_s^{(1)}i_{sq}^{(1)} + \omega_{s1}\Psi_{sd}^{(1)}\right)^2},\\ \left|\mathbf{u}_s^{(2)}\right| &= \sqrt{\left(R_s^{(2)}i_{sd}^{(2)}\right)^2 + \left(R_s^{(2)}i_{sq}^{(2)} + \omega_{s2}\Psi_{sd}^{(2)}\right)^2}.\end{aligned} \tag{11}$$

Assuming that the value of the stator winding $R_s^{(1)}$, $R_s^{(2)}$, resistance measured on both the first and second mathematical planes can be neglected for a higher power supply frequency value due to the stator reactance high value

$$\begin{aligned}X_s^{(1)} &= 2\pi f_{1h}L_s^{(1)} \gg R_s^{(1)},\\ X_s^{(2)} &= 6\pi f_{1h}L_s^{(2)} \gg R_s^{(2)},\end{aligned} \tag{12}$$

$$\left|\mathbf{u}_s^{(1)}\right| = \sqrt{\left(\omega_{s1}\Psi_s^{(1)}\right)^2}. \tag{13}$$

The nominal flux value in relative units is one for the flux of the first machine and a value of 0.2 pu for the flux of the second machine, which corresponds from 0 to 30 percent, the nominal value of the $\Psi_s^{(1)}$ flux of the V/f relationship between voltage amplitude $u_s^{(1)}$ and frequency fs for each mathematical plane (i) can be taken as:

$$|\Psi_s^{(1)}| = 1, \qquad |\Psi_s^{(2)}| = \lambda |\Psi_s^{(1)}|, \tag{14}$$

$$\frac{\left|\mathbf{u}_s^{(1)}\right|}{\omega_{s1}} = 1, \qquad \frac{\left|\mathbf{u}_s^{(2)}\right|}{\omega_{s2}} = \lambda. \tag{15}$$

The control system used to utilize the 3rd harmonic injection is well described in literature [20–24]. Orthogonal plane that rotates three times faster and in the opposite direction of the fundamental is required to take advantage of the 3rd harmonic.

## 3. CONTROL SYSTEM

In general, the slip speed of induction motors is defined as the difference between the synchronous angular speed and the rotor angular speed. The principle of this control algorithm for five-phase systems is basically the same as for three-phase systems [19]. It has implemented two independent subsystems in voltage modulation. To obtain the quasi-rectangular rotor flux distribution, the third harmonic must be injected. Therefore, fully independent control of the 1st and 3rd harmonics requires a separate control system for the 1st and 2nd mathematical planes. In order to obtain the desired quasi-rectangular resultant rotor flux distribution, the stator voltage components on the 1st and 2nd planes must be generated while maintaining synchronization with each other. This is possible due to the very flexible, fast and accurate operation of the voltage inverter. In five-phase machines, the coil shift is 72 degrees due to the number of phases. In properly adapted five-phase induction motors, increasing the saturation of the magnetic circuit can increase the rated electromagnetic torque by up to 12 [25, 26]. This is done by injecting a third harmonic into the stator supply voltage to change the shape of the flux to a quasi-rectangular one.

The drive control system operation is based on the classic solution with a slip compensation algorithm for drives with three-phase induction motors. In the presented control system, the motor feature in a five-phase configuration was used, allowing smooth, independent injection of the third harmonic into the fundamental stator supply voltage (Fig. 4). This allows you to generate an additional value of electromagnetic driving torque, allowing slip compensation in cases of high motor load.

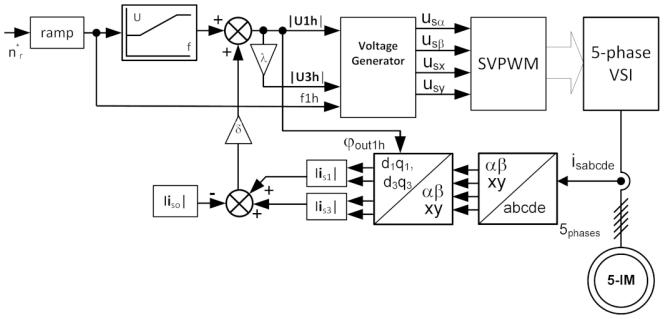


**Fig. 4.** Schematic diagram of the drive system with five-phase induction motor

The $|i_{so}|$ parameter corresponds to the stator current value for the motor without braking torque load. If the current cannot be measured, a conventional value of 40–50% of the rated motor current can be assumed. It is worth mentioning that incorrect slip compensation settings can lead to a higher DC-link voltage or instability of drive work.

The $\delta$ coefficient is selected to obtain stiff mechanical characteristics of the drive and depends strictly on the motor design and, more precisely, air gap field distribution [27–29]. The value of the $\lambda$ coefficient determines the amount of magnetic flux deformation caused by the additional 3rd voltage harmonic added to the motor supply fundamental voltage [14, 30, 31]. However, this section presents the authors' contribution to the slip compensation technique in the five-phase machine. The five-phase induction motor model is basically the same as the three-phase induction motor approach, but implemented for two independent subsystems. The drive system has been implemented on the simulation platform for power electronic and electric drive systems simulation PLECS. Figure 3 shows the structure of the system model. The operation of the electric drive was simulated using different cases of the slip compensation algorithm. Fig-

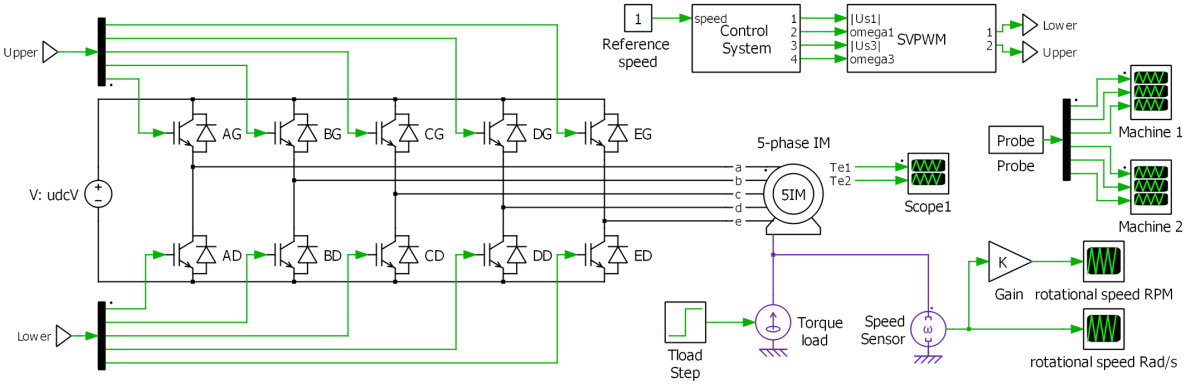


**Fig. 3.** Schematic diagram of the simulation drive system with five-phase induction motor

ure 5 shows a selected result of changes in the dynamics of the drive system with slip compensation at the rated motor speed. At time $t_1$, the motor was loaded with braking torque, and then at time $t_2$, the slip compensation algorithm was started. The algorithm operation forced an additional increase in the voltage value of the first harmonic and injection of the third harmonic of the stator supply voltage components ($u_{s\alpha}, u_{s\beta}$). As a result, the instantaneous value of the stator current increased, which can be seen by increasing the length of the vector modules of the first $|i_{s1h}|$ and third $|i_{s3h}|$ harmonic of the current. The algorithm's operation reduced the motor slip by a value equal to 0.02. The simulation results illustrate the significant potential of motor slip compensation using an additional third harmonic in the stator supply voltage. The following section describes in detail the results of synthetic laboratory tests.

The parameters of the five-phase induction motor for the first and second mathematical planes are presented in Appendix in Table 1.

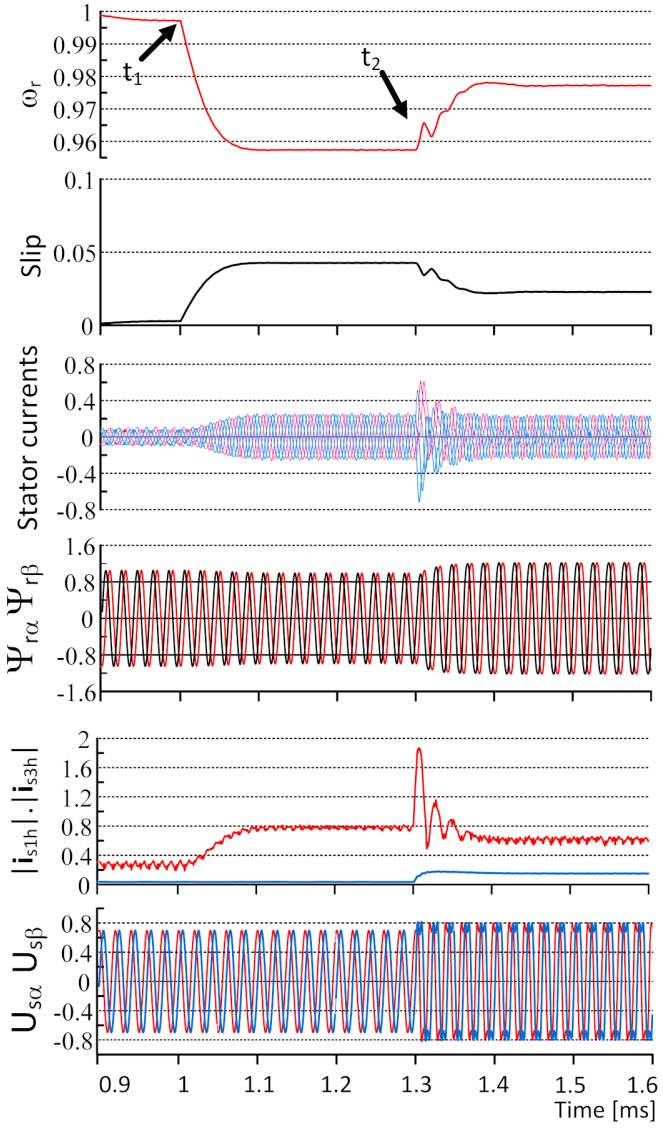


**Fig. 5.** The simulation of the five-phase induction motor dynamic with slip compensation

## 4. LABORATORY TESTS

Laboratory tests were divided into a few parts. The first part investigated the effect of the harmonic injection amplitude on the change in the motor slip value depending on the load value and low speed 0.3 pu. The second part presents the effect of the harmonic injection amplitude on speed of 0.7 pu. Finally, the simultaneous load switching and harmonics injection has been the subject of investigation.

To further verify the accuracy of the proposed method, experiments were conducted on the platform constructed in the laboratory. The PWM modulator utilizes the calculated phase voltages to generate PWM signals for a five-phase voltage source inverter. The inverter, which supplies power to the motor, generates sinusoidal, balanced voltages. The drive increases its output voltage to the maximum output voltage as a function of the DC link voltage and output frequency only when the maximum output voltage is reached. To validate the proposed control method, the dedicated algorithm was implemented using a developed five-phase inverter.

The initial laboratory test was performed with a non-load motor, 0.3 pu of motor speed and the injection of a 10% and 30% of 3rd harmonic value. The operation with the third harmonic injection presents a significant challenge due to the necessity of synchronizing with the fundamental. Moreover, it is possible to operate at a reduced speed with a third harmonic injection, and the resulting rotor flux distribution remains consistent throughout the duration of the test. As illustrated in Fig. 6, incorporating in time ($t_1$) the 10% third harmonic does not influence the slip, whereas the minimum impact of the third harmonic is 30% of the third harmonic, where $u_{s1h\alpha}$ and $u_{s3h\alpha}$ are voltage components for 1st and 3rd harmonics, and $u_{s\alpha}$ is voltage component treated as a sum of 1 and 3 voltage components, $i_{ma}$ is stator phase current. Nevertheless, the injection of the third harmonic of 30% value when the motor is under load has improved slip compensation by approximately 10% (Fig. 7).

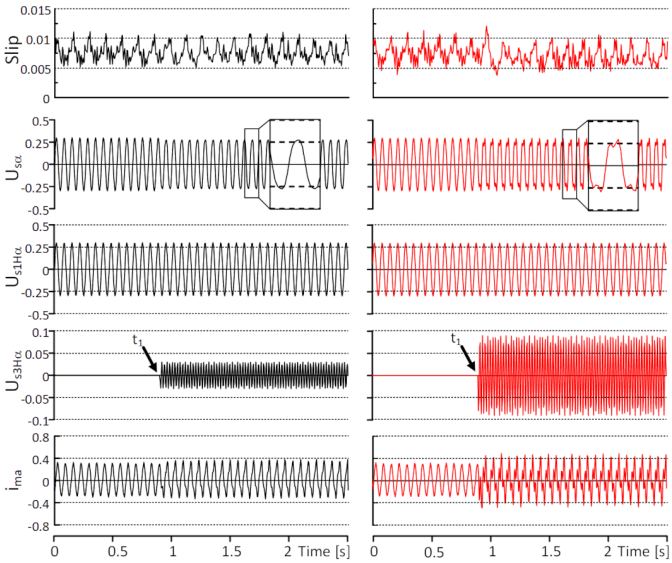


**Fig. 6.** Injection of 3rd harmonic for non-load motor with 10% (left) and 30% (right) of 3rd harmonic value. Motor speed is 0.3 pu

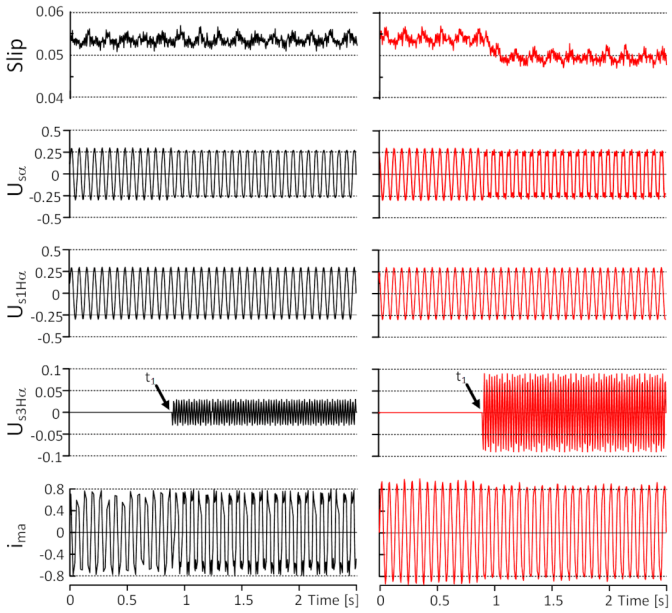


**Fig. 7.** Injection of 3rd harmonic for load motor with 10% and 30% of 3rd harmonic value. Motor speed is 0.3 pu

To more clearly demonstrate the slip compensation associated with the injection of the third harmonic, a series of steps was conducted. Figure 8 shows the test when a step load is switched on ($t_1$) and then the third harmonic of 30% value is injected ($t_2$). Enhancements in slip compensation are discernible. Figure 11 shows the time waveform of selected phase currents in injecting the 3rd harmonic of voltage into the fundamental motor supply voltage registered in the oscilloscope Tektronix MSO46. The current waveform before time $t_1$ corresponds to the motor operating at a slip of 0.97. Activation on the third harmonic of the voltage reduced the slip value to 0.98.

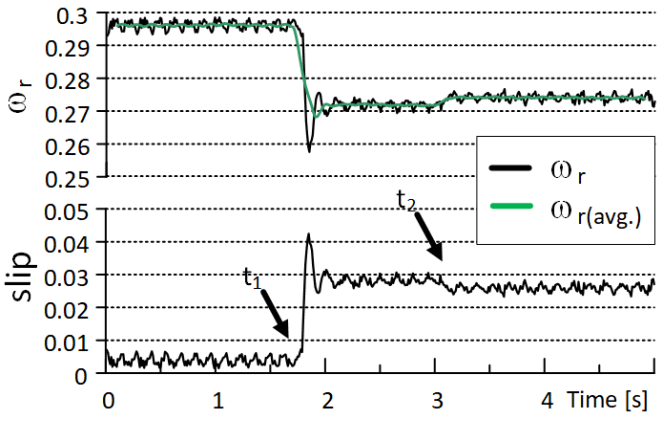


**Fig. 8.** Step load motor and 3rd harmonic injection test

The next part of laboratory tests was performed with 0.7 pu of motor speed and under the load (Fig. 9). As in the previous test, the third harmonic of 30% was injected at time $t_1$. The time waveforms show the slip, the components of the voltage vectors in the alpha axis for the first $u_{s1H\alpha}$ and second $u_{s3H\alpha}$ mathematical planes, respectively, and the sum of the voltage components $u_{s1\alpha}$ in the alpha axis in the stationary reference frame connected with the stator. The slip compensation is improved. However, compared to the speed of 0.3 pu, the compensation is not as significant as expected despite the same load value. It is evident that enhancements in slip compensation are occurring. However, in comparison with 0.3 pu of speed, the compensation is not as significant as would be expected despite the same load value.

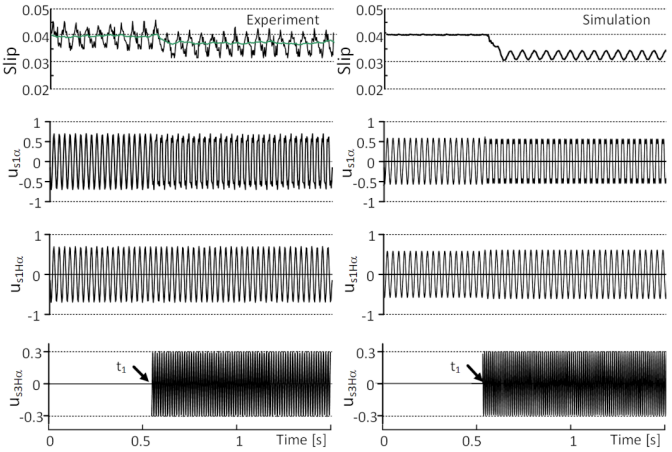


**Fig. 9.** Injection of the 3rd harmonic for load motor with 30% of the 3rd harmonic value. Motor speed is 0.7 pu

Finally, the investigation of the simultaneous injection of the 1st and 3rd harmonics under the motor step load has now been tested and the results are presented (Fig. 10). In $t_1$ the load is applied, in $t_2$ the injection on 1st harmonic of 10% of fundamental and in $t_3$ the injection on 3rd harmonic 30%. As has been expected the overall slip has been almost reduced (improved).

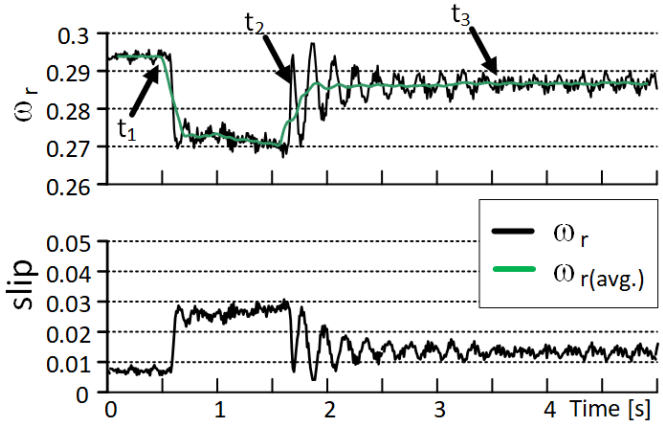


**Fig. 10.** Simultaneous injection of the 1st and 3rd harmonics under a motor step load

## 5. CONCLUSIONS

The paper presented a modified classic slip compensation method for scalar ($V/f$) control for a five-phase induction motor using a third voltage harmonic injection. This open-loop scalar

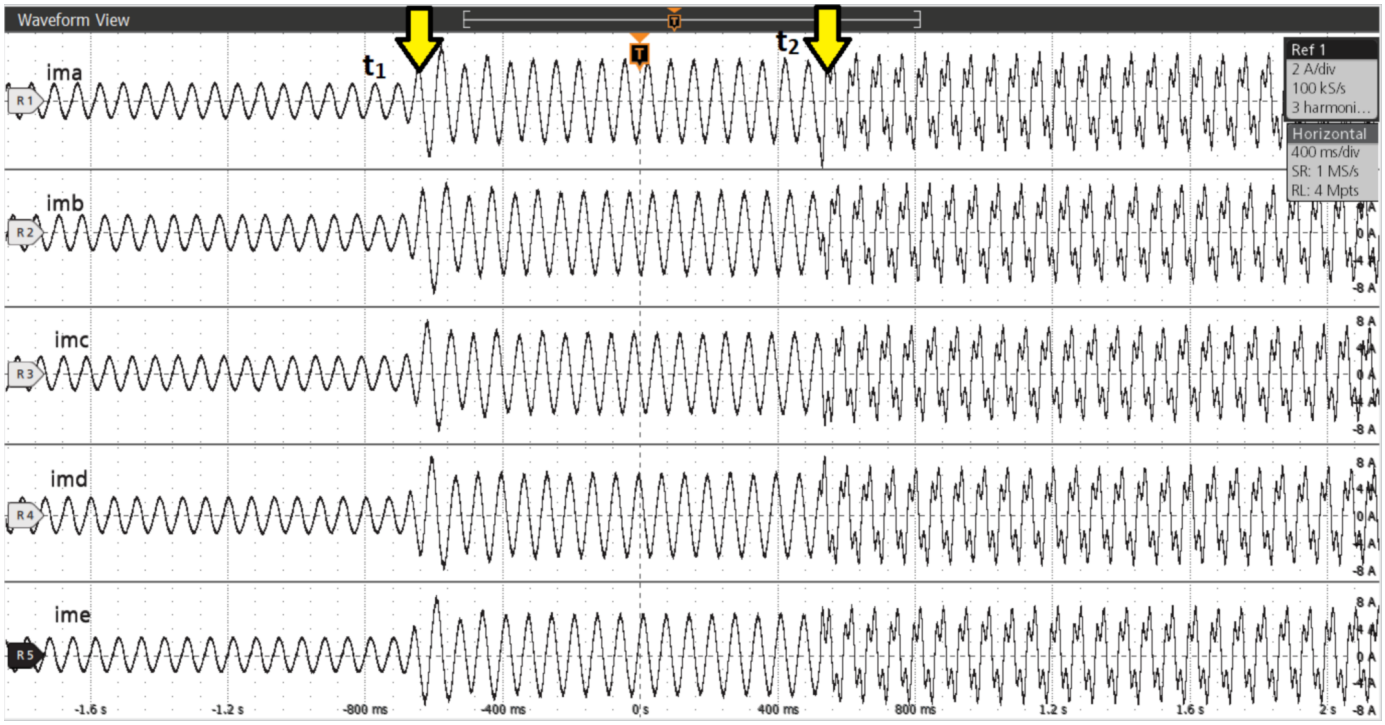


**Fig. 11.** Stator currents time waveforms during the step load and third harmonic injection tests

drive control method allows the five-phase motor to be controlled only in the drive steady state. The selection of the $\delta$ and $\lambda$ coefficients in the control system structure depend strongly on the air gap magnetic flux distribution assumed at the machine design stage. Therefore, for the purposes of conducting laboratory tests with a particular prototype of a five-phase motor, these values were selected on the basis of experimental evidence.

The paper presents the simulation results and describes the laboratory tests that were conducted. The several scenarios were performed in a laboratory stand using a five-phase induction motor. As has been predicted the injection of the 1$^{st}$ and especially 3$^{rd}$ harmonics has resulted in a reduction in slip. The degree of slip was compensated for by a factor of 5% to 10%, contingent upon the specific test. Nevertheless, the profitability of this approach is contingent upon certain circumstances, as the injection of harmonics is not a universal solution. At lower speeds, there is the potential for markedly superior results to be achieved. Moreover, this solution is more beneficial when the motor is loaded with a torque close to the rated torque. The injection of a third harmonic into the stator voltage allows for a wider utilization of the stator magnetic circuit. This is achieved through the incorporation of a 2$^{nd}$ plane that synchronizes the stator flux. However, when using this solution, it is essential to consider the increase in losses in the motor magnetic circuit due to the presence of strongly distorted currents.

## ACKNOWLEDGEMENTS

This work was supported by the National Centre for Research and Development and Lider Program under Grant no. LIDER13/0153/2022.

## APPENDIX

Table 1 presents the parameters of the prototype of a five-phase induction motor used for laboratory tests. Figure 12 shows a configuration of the laboratory setup with the analysed five-phase motor coupled with three three-phase load motors. The prototype of a five-phase voltage source inverter supplies the analysed five-phase induction motor in an electric drive shaft.

**Table 1**
Five-pahse induction motor parameters

| Symbol | Parameter | Value |
|---|---|---|
| $P_n$ | IM nominal power | 5.5 kW |
| $\omega_n$ | Rated speed | 1420 rpm |
| $I_n$ | Rated current | 8.8 |
| $f_n$ | Rated stator frequency | 50 Hz |
| $R_s^{(1)}$ | Stator resistance 1$^{st}$ plane | 1.04 Ω |
| $R_r^{(1)}$ | Rotor resistance 1$^{ST}$plane | 1.69 Ω |
| $L_s^{(1)}$ | Stator leakage inductance 1$^{st}$ plane | 11 mH |
| $L_r^{(1)}$ | Rotor leakage inductance 1$^{st}$ plane | 11 mH |
| $L_m^{(1)}$ | Magnetization inductance 1$^{st}$ plane | 286 mH |
| $R_s^{(2)}$ | Stator resistance 2$^{nd}$ plane | 1.04 Ω |
| $R_r^{(2)}$ | Rotor resistance 2$^{nd}$ plane | 2.56 Ω |
| $L_s^{(2)}$ | Stator leakage inductance 2$^{nd}$ plane | 9 mH |
| $L_r^{(2)}$ | Rotor leakage inductance 2$^{nd}$ plane | 9 mH |
| $L_m^{(2)}$ | Magnetization inductance 2$^{nd}$ plane | 48 mH |

**Fig. 12.** Laboratory stand with five-phases induction motor (left) and induction motor emulated the load (right)

## REFERENCES

[1] R.H. Byrne, T.A. Nguyen, D.A. Copp, B.R. Chalamala, and I. Gyuk, "Energy management and optimization methods for grid energy storage systems," *IEEE Access*, vol. 6, pp. 13 231–13 260, Aug. 2017, doi: 10.1109/ACCESS.2017.2741578.

[2] M. Adamczyk and T. Orlowska-Kowalska, "Influence of the stator current reconstruction method on direct torque control of induction motor drive in current sensor postfault operation," *Bull. Pol. Acad. Sci. Tech. Sci.*, vol. 70, p. e140099, 2022, doi: 10.24425/BPASTS.2022.140099.

[3] S. Jain, A.K. Thopukara, R. Karampuri, and V.T. Somasekhar, "A single-stage photovoltaic system for a dual-inverter-fed open-end winding induction motor drive for pumping applications," *IEEE Trans. Power Electron.*, vol. 9, pp. 4809–4818, Sep. 2015, doi: 10.1109/TPEL.2014.2365516.

[4] E. Robles, M. Fernandez, J. Andreu, E. Ibarra, J. Zaragoza, and U. Ugalde, "Common-mode voltage mitigation in multiphase electric motor drive systems," *Renew. Sustain. Energy Rev.*, vol. 157, p. 111971, Apr. 2022, doi: 10.1016/J.RSER.2021.111971.

[5] G. Brando, A. Dannier, and I. Spina, "A full order sensorless control adaptive observer for doubly-fed induction generator," in *ICCEP 2019 – 7th International Conference on Clean Electrical Power: Renewable Energy Resources Impact*. Institute of Electrical and Electronics Engineers Inc., Jul. 2019, pp. 464–469, doi: 10.1109/ICCEP.2019.8890195.

[6] E. Fedele, D. Lauria, and R. Rizzo, "Dfig capability under weak grid connection and different reactive power control modes," in *2023 International Conference on Clean Electrical Power, ICCEP 2023*, 2023, pp. 896–902, doi: 10.1109/ICCEP57914.2023.10247462.

[7] A. Glowacz *et al.*, "Fault diagnosis of electrical faults of three-phase induction motors using acoustic analysis," *Bull. Pol. Acad. Sci. Tech. Sci.*, vol. 72, p. e148440, 2024, doi: 10.24425/BPASTS.2024.148440.

[8] R. Kumar and B. Singh, "Bldc motor-driven solar pv array-fed water pumping system employing zeta converter," *IEEE Trans. Ind. Appl.*, vol. 52, pp. 2315–2322, May 2016, doi: 10.1109/TIA.2016.2522943.

[9] R. Ryndzionek, K. Blecharz, F. Kutt, M. Michna, and G. Kostro, "Development and performance analysis of a novel multiphase doubly-fed induction generator," *Arch. Electr. Eng.*, vol. 71, pp. 1003–1015, 2022, doi: 10.24425/AEE.2022.142121.

[10] A.S. Nanoty and A.R. Chudasama, "Design of multiphase induction motor for electric ship propulsion," in *2011 IEEE Electric Ship Technologies Symposium (ESTS 2011)*, 2011, pp. 283–287, doi: 10.1109/ESTS.2011.5770882.

[11] P. Maciejewski and G. Iwański, "Six-phase doubly fed induction machine-based standalone dc voltage generator," *Bull. Pol. Acad. Sci. Tech. Sci.*, vol. 69, p. e135839, 2021, doi: 10.24425/BPASTS.2021.135839.

[12] K. Kyslan, M. Lacko, Ž. Ferková, V. Petro, S. Padmanaban, and D. Perduková, "Current limitation method for v/f control of five-phase induction machines," *Int. Trans. Electr. Energy Syst.*, vol. 2022, p. 5165666, 2022, doi: 10.1155/2022/5165666.

[13] M. Hinkkanen, L. Tiitinen, E. Molsa, and L. Harnefors, "On the stability of volts-per-hertz control for induction motors," *IEEE J. Emerg. Sel. Top. Power Electron.*, vol. 10, pp. 1609–1618, Apr. 2022, doi: 10.1109/JESTPE.2021.3060583.

[14] A.S. Abdel-Khalik, M.I. Masoud, and B.W. Williams, "Improved flux pattern with third harmonic injection for multiphase induction machines," *IEEE Trans. Power Electron.*, vol. 27, pp. 1563–1578, 2012, doi: 10.1109/TPEL.2011.2163320.

[15] P. Strankowski, J. Guzinski, M. Morawiec, A. Lewicki, and F. Wilczynski, "Sensorless five-phase induction motor drive with third harmonic injection and inverter output filter," *Bull. Pol. Acad. Sci. Tech. Sci.*, vol. 68, pp. 437–445, Jun. 2020, doi: 10.24425/BPASTS.2020.133369.

[16] K. Łuksza, D. Kondratenko, and A. Lewicki, "Dead time effects compensation strategy by third harmonic injection for a five-phase inverter," *Arch. Electr.l Eng.*, vol. 73, pp. 17–35, 2024, doi: 10.24425/AEE.2024.148854.

[17] M. Morawiec and P. Kroplewski, "Nonadaptive estimation of the rotor speed in an adaptive full order observer of induction machine," *Bull. Pol. Acad. Sci. Tech. Sci.*, vol. 68, pp. 973–981, Oct. 2020, doi: 10.24425/BPASTS.2020.134654.

[18] T. Białoń, A. Lewicki, M. Pasko, and R. Niestrój, "Parameter selection of an adaptive pi state observer for an induction motor," *Bull. Pol. Acad. Sci. Tech. Sci.*, vol. 61, pp. 599–603, Sep. 2013, doi: 10.2478/BPASTS-2013-0062.

[19] M. Morawiec, P. Strankowski, A. Lewicki, and J. Guzinski, "Sensorless control of five-phase induction machine supplied by the vsi with output filter," in *Proc. 2016 10th International Conference on Compatibility, Power Electronics and Power Engineering, CPE-POWERENG 2016*, Aug. 2016, pp. 304–309, doi: 10.1109/CPE.2016.7544204.

[20] P. Strankowski, J. Guziński, F. Wilczyński, M. Morawiec, and A. Lewicki, "Open-phase fault detection method for sensorless five-phase induction motor drives with an inverter output filter," *Power Electron. Drives*, vol. 4, no. 1, pp. 191–202, 2019, doi: 10.2478/pead-2019-0004.

[21] P. Zhu, M. Qiao, Y. Wei, and Y. Xia, "Research on five-phase induction motor system control with third harmonic current injection," *J. Eng.*, vol. 2017, pp. 2559–2563, Jan. 2017, doi: 10.1049/JOE.2017.0789.

[22] A. Ray, S. Belkhode, R. Karampuri, and S. Jain, "Optimized pwm techniques with 3rd harmonic injection for five phase concentrated winding induction motor with open-end stator," in *Proc. 2018 IEEE International Conference on Power Electronics, Drives and Energy Systems, PEDES 2018*, Jul. 2018, doi: 10.1109/PEDES.2018.8707549.

[23] R.O.C. Lyra and T.A. Lipo, "Torque density improvement in a six-phase induction motor with third harmonic current injec-

tion," *IEEE Trans. Ind. Appl.*, vol. 38, pp. 1351–1360, 2002, doi: 10.1109/TIA.2002.802938.

[24] M.R. Arahal, M.J. Duran, F. Barrero, and S.L. Toral, "Stability analysis of five-phase induction motor drives with variable third harmonic injection," *Electr. Power Syst. Res.*, vol. 80, pp. 1459–1468, Dec. 2010, doi: 10.1016/J.EPSR.2010.06.011.

[25] W. Yu, X. Liu, and W. Kong, "Torque density improvement for five-phase induction motor drive with harmonic current injection in electric vehicles application," in *ICEMS 2018 – 2018 21st International Conference on Electrical Machines and Systems*, Nov. 2018, pp. 2525–2528, doi: 10.23919/ICEMS.2018.8549474.

[26] P. Zhao and G. Yang, "Torque density improvement of five-phase pmsm drive for electric vehicles applications," *J. Power Electron.*, vol. 11, pp. 401–407, 2011, doi: 10.6113/JPE.2011.11.4.401.

[27] W. Kong, R. Qu, J. Huang, and M. Kang, "Air-gap and yoke flux density optimization for multiphase induction motor based on novel harmonic current injection method," in *Proc. 2016 22nd International Conference on Electrical Machines, ICEM 2016*, Nov. 2016, pp. 100–106, doi: 10.1109/ICELMACH.2016.7732512.

[28] H. Liu, D. Wang, X. Yi, X. Zheng, X. Yu, and B. Pan, "Loss reduction of five-phase induction motor with third harmonic injection throughout widest torque range under open-circuit faults," *IEEE J. Emerg. Sel. Top. Power Electron.*, vol. 11, pp. 4643–4658, Oct. 2023, doi: 10.1109/JESTPE.2023.3300367.

[29] A.G. Yepes, A. Shawier, W.E. Abdel-Azim, A.S. Abdel-Khalik, S. Ahmed, and J. Doval-Gandoy, "General online current-harmonic generation for increased torque capability with minimum stator copper loss in fault-tolerant multiphase induction motor drives," *IEEE Trans. Transp. Electrif.*, vol. 9, pp. 4650–4667, Sep. 2023, doi: 10.1109/TTE.2023.3244742.

[30] C.C. Scharlau, L.F.A. Pereira, L.A. Pereira, and S. Haffner, "Performance of a five-phase induction machine with optimized air gap field under open loop v/f control," *IEEE Trans. Energy Convers.*, vol. 23, pp. 1046–1056, 2008, doi: 10.1109/TEC.2008.2001437.

[31] H. Hussain, G. Yang, R. Deng, and J. Yang, "Harmonic injection strategy considering multiplane iron loss impact with optimal magnetizing flux distribution for multiphase induction machines," *IEEE Trans. Ind. Electron.*, vol. 70, pp. 6530–6539, Jul. 2023, doi: 10.1109/TIE.2022.3203683.